



PERGAMON

Solid State Communications 125 (2003) 185–188

**solid
state
communications**

www.elsevier.com/locate/ssc

High-density uniformly aligned silicon nanotip arrays and their enhanced field emission characteristics

X.D. Bai^{a,b}, C.Y. Zhi^a, S. Liu^a, E.G. Wang^{a*}, Z.L. Wang^{b,*}

^aInternational Center for Quantum Structures and State Key Laboratory for Surface Physics, Chinese Academy of Sciences, Beijing 100080, People's Republic of China

^bSchool of Materials Science and Engineering, Georgia Institute of Technology, 771 Ferst Dr, Atlanta, GA 30332-0245, USA

Received 24 August 2002; accepted 30 October 2002 by D. Van Dyck

Abstract

High-density ($\sim 10^8/\text{cm}^2$), uniformly aligned silicon nanotip arrays are synthesized by a plasma-assisted hot-filament chemical vapor deposition process using mixed gases composed of hydrogen, nitrogen and methane. The silicon nanotips grow along (112), and are coated in situ with a ~ 3 nm thick amorphous carbon film by increasing the methane concentration in the source gases. In comparison to the uncoated silicon nanotips arrays, the coated tips have enhanced field emission properties with a turn-on field of $1.6 \text{ V}/\mu\text{m}$ (for $10 \mu\text{A}/\text{cm}^2$) and threshold field of $3 \text{ V}/\mu\text{m}$ (for $10 \text{ mA}/\text{cm}^2$), suggesting their potential applications for flat panel displays.

© 2003 Elsevier Science Ltd. All rights reserved.

PACS: 81.05.Zx; 81.15.Gh; 79.70.+Q

Keywords: A. Semiconductor; D. Electronic transport

Silicon nanotip arrays are of great interest due to a wide variety of applications in vacuum microelectronic and optoelectronic devices, flat panel displays [1] and semiconductor field emitting [2–4]. As a field emitter array, silicon tips are required to be small in size and uniformly distributed, and have high density at large scale. Lithographical technique is normally employed to produce silicon tip arrays, by which the tips with small sizes, even below 10 nm in diameter, can be obtained [5,6] although the fabrication process is expensive. Nanoscale silicon cones covering a large surface area can be prepared by using metal films as the plasma etching mask [7,8], but the heights and apex angles of the cones have a wide distribution. The microsize silicon tips are usually obtained by traditional methods of vapor-liquid-solid (VLS) growth process and chemical etching. It is, therefore, still a challenge to produce cost-effective nanosize silicon tip arrays for practical applications.

Much effort has been devoted to coating silicon tip/cone arrays in order to improve their field emission properties. Evtukh et al. [9] made the silicon tip arrays coated with nanocomposite films. Wong et al. [10] fabricated the silicon cone arrays with cesium coating. Nagao et al. [11] deposited NbN_x thin film on the silicon cone arrays. Many other researchers have also studied the effect of diamond coating on silicon tip arrays [12–14]. But for all of these approaches, the thickness of the coating layer is rather difficult to control, which is important in determining their field emission properties.

In this letter, high-density uniform silicon nanotip arrays have been fabricated by a plasma-assisted hot-filament chemical deposition (HFCVD) process. By increasing methane concentration in the source gases, the silicon nanotips are coated in situ by thin amorphous carbon film, which largely enhanced their field emission performance.

The details on the HFCVD system was described previously [15,16]. In brief, a dc power supply ($630 \text{ V} \times 1 \text{ A}$) was used to generate discharge plasma between the tantalum base (cathode) and a tantalum plate installed above a deeply carbonized tungsten filament ($\phi = 0.3 \text{ mm}$). Polished Si

* Corresponding authors. Tel.: 404-894-8008; fax: 404-894-9140.

E-mail addresses: zhong.wang@mse.gatech.edu (Z.L. Wang), egwang@aphy.iphys.ac.cn (E.G. Wang).

(100) wafers (10 mm × 10 mm) were used as substrates. The filament was heated to about 190 °C. A negative bias of 600 V was applied to generate a plasma of about 25 mA/cm² in intensity. The filament was used to assist dissociation of the inlet gases and generation of the plasma, which plays a key role in the sputtering of silicon substrate and re-deposition of the silicon atoms. The substrate temperature was maintained at about 850 °C. A mixture of hydrogen (99.999% purity), nitrogen (99.999% purity) and methane (99.9% purity) were used as the source gas. The gas flow rate was 100 sccm and the work pressure was kept at 4.0 kPa during the entire growth process (2 h). The flow rate ratio between hydrogen and nitrogen were kept at 3:1. The concentration (vol.%) of methane was changed from 10 to 3% for the fabrication of silicon tips with and without in situ carbon coating, respectively. The morphology of the as-synthesized films was characterized by scanning electron microscopy (LEO 1530 FEG SEM). The microstructure and chemical compositions of the samples were determined by high-resolution transmission electron microscopy (Hitachi HF-2000 FEG TEM) and the energy dispersive X-ray spectroscopy (EDS) and electron energy-loss spectroscopy (EELS).

Fig. 1(a) is a SEM image of a sample tilted 30° angle from its normal, showing a large-area silicon nanotip array.

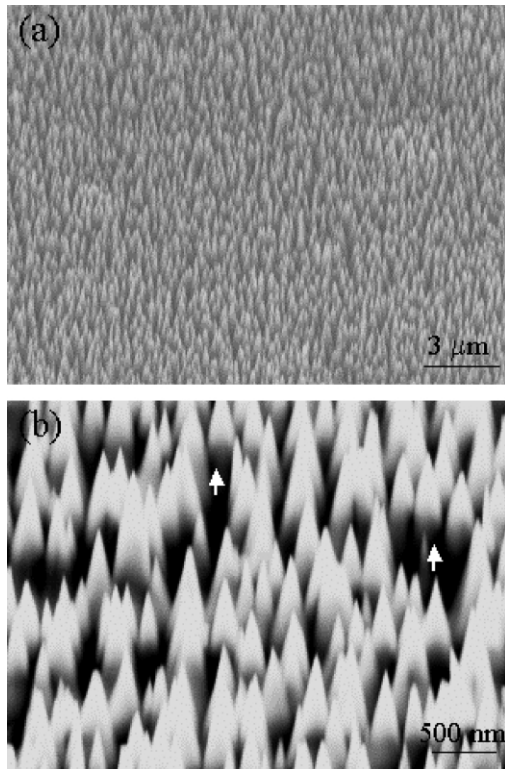


Fig. 1. SEM images recorded at 30° angle from the substrate normal, (a) showing the large-scale uniform silicon nanotip array, and (b) the structural uniformity in size, apex angle and distribution.

The tips are very uniform in both height and apex angle. The distribution of the tips is also very uniform. The density of the tips is estimated to be about 10⁸/cm², which is one to two orders of magnitude higher than that reported previously [17]. The detailed information of the nanotips can be captured through high-magnification SEM image, as shown in Fig. 1(b). The tips are 400–500 nm in height and the average apex angle of the tips are ~22° after making the correction of the 30° view angle with the substrate normal. The diameters at the bottom of the tips are 200–300 nm. In the area of wider separations among tips, as indicated by arrowheads, the cone-shaped tips grow on well-aligned cylindrical pillars, which is a distinctive feature of our sample. This kind of nanotips may also serve as the tips for scanning probe microscopy. The formation of uniformly aligned nanotips maybe resulted from re-deposition of silicon together with plasma etching.

The characterization of silicon nanotips by TEM is shown in Fig. 2. The tip is very sharp. The selected area electron diffraction pattern, inset in Fig. 2(a), reveals that the tips are single crystalline with diamond structure. Fig. 2(b) is an EDS spectrum of the nanotip, which further confirms that the sample is pure silicon. The growth direction of the tip is $\langle 112 \rangle$, and the apex angle as viewing along $[1\ 1\ \bar{1}]$ is measured to be $22 \pm 1^\circ$ based on both TEM and SEM images. The side surfaces of the tip given in Fig. 2(a) are determined from the electron diffraction pattern to be $(4\ \bar{5}\ \bar{1})$ and $(5\ \bar{4}\ 1)$, which have an angle of 21.78° , in excellent agreement with the measured apex angle.

By increasing the methane concentration in precursor to 10 vol.%, the nanotip arrays, with similar density and uniformity as those shown in Fig. 1, can also be fabricated. The most interesting feature is that there is a thin and uniform film of carbon directly deposited onto the nanotip surface (Fig. 3(a)). The high-resolution TEM image from

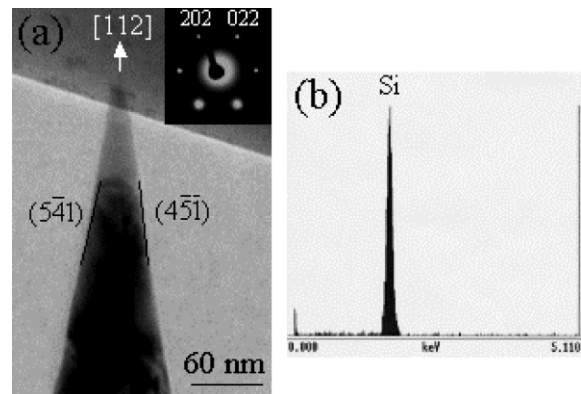


Fig. 2. (a) TEM image of a silicon nanotip, and the corresponding electron diffraction pattern, (b) and the EDS spectrum. The nanotip was grown with 3% CH₄, showing no carbon passivation on the surface. The nanotip is oriented with $[1\ 1\ \bar{1}]$ parallel to the electron beam, its growth direction is $[112]$, and its side surfaces are $(4\ \bar{5}\ \bar{1})$ and $(5\ \bar{4}\ 1)$.

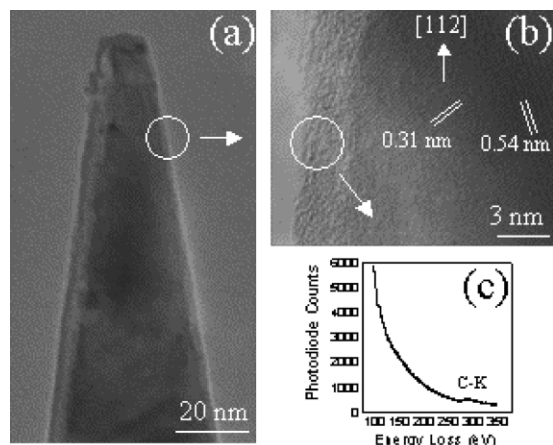


Fig. 3. (a) TEM image of a silicon nanotip coated with a thin carbon film, (b) a high-resolution TEM image from the edge showing ~ 3 nm thick amorphous carbon film on the surface. (c) EELS spectrum acquired from the surface coating film. The nanotip was grown with 10% CH_4 , showing a thin layer of carbon passivation on the surface.

the edge of the tip (circled in Fig. 3(a)) is shown in Fig. 3(b), which indicates that the silicon tip is coated by ~ 3 nm thick amorphous film. Nanoprobe EELS was used to analyze the composition of the passivation layer on the nanotip. As shown in Fig. 3(c), there is a clear C k-edge peak, and no obvious Si peak was detected. We have also extended the EELS energy scope, there is no indication that the presence of oxygen at 532 eV. Therefore, the coating is amorphous carbon film.

The field emission characteristics of the silicon nanotip array with and without carbon coating were investigated at room temperature in a vacuum chamber of 10^{-6} Pa. The sample was used as the cathode, and a molybdenum probe with 1.5 mm in diameter was acted as the anode. In this study, the vacuum gap between anode and sample was set to be 1 mm. The applied voltage ranged from 300 V to 15 kV, and the emission current was measured by a picoampere meter (Keithley 485).

Fig. 4(a) shows the current density versus the electric field (I – V) characteristics for the silicon nanotip arrays with and without amorphous carbon layer. The large field emission enhancement for silicon nanotip array was achieved by its carbon layer coated in situ. Using the classical definitions of E_{to} (turn-on field) and E_{thr} (threshold field) to be the electrical fields needed to produce a current of $10 \mu\text{A}/\text{cm}^2$ and $10 \text{mA}/\text{cm}^2$, respectively, E_{to} and E_{thr} are 1.6 and 3 $\text{V}/\mu\text{m}$ for the silicon nanotip arrays with carbon coating. Both parameters are even lower than those of well-aligned carbon nanotube emitter arrays [18–20]. The enhanced field emission performance of silicon nanotip arrays with carbon coating is attributed to the uniform coverage of carbon onto the sharp nanotips. One should note that, different from carbon nanotubes, there is no field-emission influence from metal catalyst particles on the

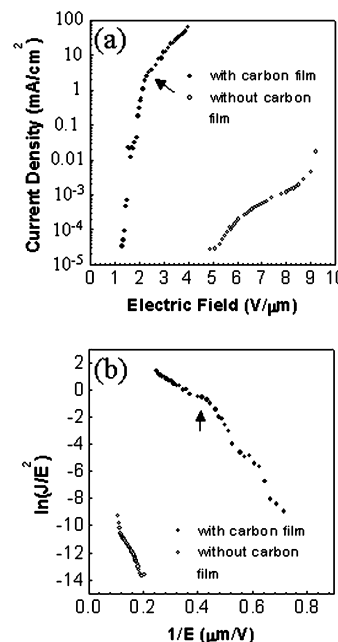


Fig. 4. (a) Field-emission current density vs electric field for silicon nanotip arrays with and without carbon coating. (b) Corresponding F–N plots. The arrowheads indicate the onset of saturation.

nanotips. Fig. 4(b) shows the Fowler–Nordheim (F–N) plots of the same emission data presented in Fig. 4(a). The F–N slope for the nanotips without carbon coating shows the typical characteristics of field emission from semiconductors [21]. The F–N plot of the array with amorphous carbon layers can be fitted to straight lines in two regimes, and displays an onset field near 2.5 $\text{V}/\mu\text{m}$, as indicated by an arrowhead in Fig. 4(a).

The HFCVD system used in our experiments is relatively simple, cost-effective, and can be easily expanded to produce large-size high-quality nanotip arrays. It is important to point out that a new feature in our process is the ability of producing in situ carbon coating onto the silicon tips with a uniform coverage, which has been demonstrated to be the key for enhancing the field emission properties. This process avoids the complexity of post coating treatments as in conventional approaches. The coated carbon film also has the advantage of preventing surface from oxidation, and the sample possesses the equivalent merits of carbon nanotip arrays [22,23]. Therefore, the silicon nanotip arrays with in situ carbon film coating are promising candidates for applications in flat panel display, semiconductor field emitters, and possibly as nano-needles for biomedical drug delivery.

Acknowledgements

This work was supported by NSF of China, Chinese

Academy of Sciences, National Key Project for Basic Research (G2000067103).

References

- [1] E.I. Givargizov, V.V. Zhirmov, N.N. Chubun, A.N. Stepanova, *J. Vac. Sci. Technol. B* 15 (1997) 450.
- [2] K.L. Jensen, Y.Y. Lau, D. McGregor, *Solid-State Electron.* 45 (2001) 831.
- [3] D.R. Whaley, B. Gannon, C.R. Smith, C.M. Armstrong, C.A. Spindt, *IEEE Trans. Plasma. Sci.* 28 (2000) 727.
- [4] K.L. Jensen, Y.Y. Lau, D. McGregor, *Appl. Phys. Lett.* 77 (2000) 585.
- [5] E. Gogolides, S. Grigoropoulos, A.G. Nassiopoulos, *Microelectron. Engng* 27 (1995) 449.
- [6] W. Chen, H. Ahmed, *Appl. Phys. Lett.* 63 (1993) 1116.
- [7] K. Seeger, R.E. Palmer, *Appl. Phys. Lett.* 74 (1999) 1627.
- [8] T. Tada, T. Kanayama, K. Koga, K. Seeger, S.J. Carroll, P. Weibel, E. Palmer, *Microelectron. Engng* 41/42 (1998) 539.
- [9] A.A. Evtukh, E.B. Kaganovich, V.G. Litovchenko, Y.M. Litvin, D.V. Fedin, E.G. Manoilov, S.V. Svechnikov, *Mater. Sci. Engng C* 19 (2002) 401.
- [10] W.K. Wong, F.Y. Meng, Q. Li, F.C.K. Au, I. Bello, S.T. Lee, *Appl. Phys. Lett.* 80 (2002) 877.
- [11] M. Nagao, Y. Gotoh, T. Ura, H. Tsuji, J. Ishikawa, *J. Vac. Sci. Technol. B* 17 (1999) 623.
- [12] N.S. Xu, J.C. She, S.E. Huq, J. Chen, S.Z. Deng, *Appl. Phys. Lett.* 73 (1998) 3668.
- [13] W.B. Choi, J.J. Cuomo, V.V. Zhirmov, A.F. Myers, J.J. Hren, *Appl. Phys. Lett.* 68 (1996) 720.
- [14] E.I. Givargizov, *J. Vac. Sci. Technol. B* 13 (1995) 414.
- [15] X.D. Bai, J.D. Guo, J. Yu, E.G. Wang, J. Yuan, W. Zhou, *Appl. Phys. Lett.* 76 (2000) 2624.
- [16] Y. Chen, L.P. Guo, E.G. Wang, *Philos. Mag. Lett.* 75 (1997) 155.
- [17] Y. Chen, L. Guo, D.T. Shaw, *J. Cryst. Growth* 210 (2000) 527.
- [18] S. Fan, M.G. Chapline, N.R. Franklin, T.W. Tomblor, A.M. Cassell, H. Dai, *Science* 283 (1999) 512.
- [19] H. Murakami, M. Hirakawa, C. Tanaka, H. Yamakawa, *Appl. Phys. Lett.* 76 (2000) 1776.
- [20] D. Xu, G. Guo, L. Gui, Y. Tang, Z. Shi, Z. Jin, Z. Gu, W. Liu, X. Li, G. Zhang, *Appl. Phys. Lett.* 75 (1999) 481.
- [21] G. Fursey, *Appl. Surf. Sci.* 94/95 (1996) 44.
- [22] J. Jang, S.J. Chung, H.S. Kim, S.H. Lim, C.H. Lee, *Appl. Phys. Lett.* 79 (2001) 1682.
- [23] C.L. Tsai, C.F. Chen, C.L. Lin, *Appl. Phys. Lett.* 80 (2002) 1821.